

# Calculating the Re-Entry Probability for a given Area of Interest

Jens Agena<sup>(1)</sup>, Benjamin Müller<sup>(2)</sup>

<sup>(1)</sup> DLR, Mühlenstraße 89, 47589 Uedem, Germany, Email: jens.agena@dlr.de

<sup>(2)</sup> Bundeswehr, Mühlenstraße 89, 47589 Uedem, Germany, Email: benjamin15mueller@bundeswehr.org

## ABSTRACT

Calculating re-entry predictions is part of the daily business at the German Space Situational Awareness Centre (GSSAC). An analysis mode for the re-entry propagator was developed to give the operator more information to evaluate a re-entry event.

This paper outlines the applied Monte Carlo analysis and the utilized filter technique to smooth the results. The received data can be used to calculate the re-entry probability for a given area of interest.

The new method is presented for a re-entry of a Molniya satellite from December 2016.

Key words: GSSAC, SSA, re-entry risk analyses.

## 1 INTRODUCTION

Calculating re-entry predictions always includes uncertainties related for example to errors resulting from the orbit determination process or the forecast of atmospheric density as the main driving factor for the calculations.

The application of different atmosphere models results in using a  $\pm 20\%$  window of the remaining on-orbit life time around the calculated nominal re-entry time [1]. Applying this time window attempts to match the uncertainties in the calculation but gives no further information of the re-entry probability for a certain area of interest. The aim of the introduced analysis is to calculate this remaining probability of a re-entry for a given time period and an area of interest.

For this purpose a Monte Carlo simulation is applied which results in an adequate number of re-entry time stamps for each analysis. Thus, the nominal state vector of the object is varied by using independent normal distributions for the position, the velocity and the ballistic coefficient. Subsequent to the Monte Carlo run a low-pass filter is applied to the resulting re-entry timestamps. This results in a smoothed probability distribution which is used to determine the accumulated probability.

The obtained results of the re-entry analysis can be used to provide relative re-entry probabilities for areas of interest based on generated simulation data.

### 1.1 Requirements from operations

Considering these uncertainties we experience some issues during space situational awareness (SSA) operations e.g. the problem of false alerts. If the number of false alerts is too high, people with no background in space will start to ignore warnings. Thus the requirement from operations is to minimise the number of false positive alerts.

During current operations at the German Space Situational Awareness Centre (GSSAC) this problem is being solved with a compromise: warnings are not released before the uncertainty window is below plus minus two hours, based on Tracking and Impact Predictions (TIPs) received from JSpOC. This means for most re-entering objects an uncertainty of about 2.5 orbits is applied (see Fig. 1).



Figure 1. Ground track with 100min window around center of impact window (COIW)

Fig. 1 displays the ground track of an object with a window of 100 min around the center of impact window (COIW) for our own prediction. During the remaining time of uncertainty there are still two overflights for a certain area of interest (in this case the central land mass of the EU member states). The window is derived by using a  $\pm 20\%$  window of the remaining on-orbit life time. Thus there is no information about the probability for re-entry at any position on the ground track. This means for any remaining overflight a notification will be send.

Looking at the last calculations for this object reveals the problem (see Fig. 2). The COIW was calculated one orbit revolution earlier and due to a smaller uncertainty window no more overflights for the given area of interest occur. Thus any earlier warning was a false alert.

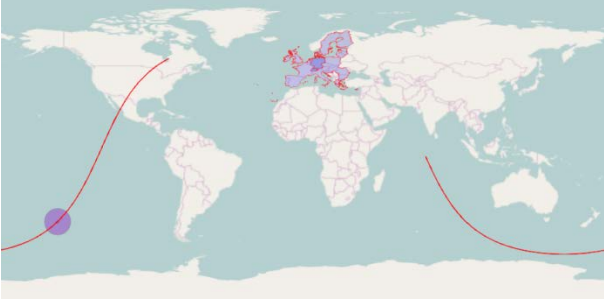


Figure 2. Ground track with 30min window around center of impact window

An analysis mode for the numeric propagator was implemented to get more information about a given re-entry. The approach was to use statistical analysis (Monte Carlo simulations) to get a probability of re-entry for a given area of interest.

## 1.2 Applying a Monte Carlo simulation

The new analysis mode of the re-entry propagator runs a variable number of Monte Carlo simulations (based on user input) by applying a variation to the initial state vector using independent normal distributions (e.g. using variance-covariance information from orbit determination). In Tab. 1 the different options for adding an error are listed.

Table 1. List of possible variations for re-entry analysis

Error	Unit	Type
satellite position	km	standard deviation
satellite velocity	km/s	standard deviation
ballistic coefficient	m <sup>2</sup> /kg	standard deviation
Solar radiation pressure coefficient	m <sup>2</sup> /kg	standard deviation

Each value can be changed independently from each other or even be turned off. This leads to a cloud of new, normal distributed, state vectors. For each of them a re-entry calculation will be performed leading to a list of re-entry time stamps and locations.

In Fig. 3 this distribution for 1000 Monte Carlo runs is shown for the same object as illustrated before. It can be seen that there are some peaks following a low frequent curve with some high frequent noise. The shape of the curve is characteristically for objects with high eccentric orbits, building peaks at any perigee pass.

There are some possibilities to reduce the influence of the noise. One could raise the number of Monte Carlo runs or apply a low-pass filter. The filter method was chosen to save computation time and because 1000 calculations already build a characteristic curve for a remaining life time less than one day.

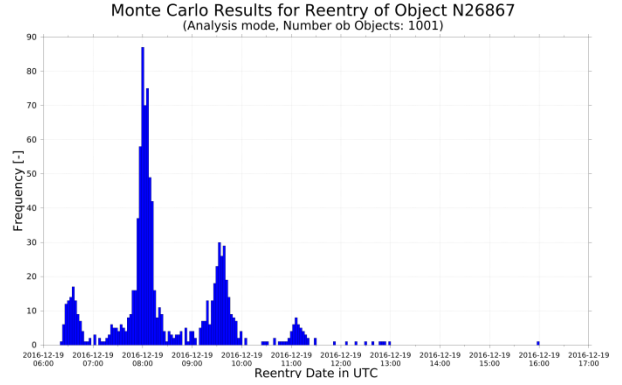


Figure 3. Distribution of re-entry time stamps

## 1.3 Utilised filter techniques

At first an adequate filter has to be chosen. The main requirements for this filter are a short calculations time and that the filter must have no negative part to prevent the appearance of negative probability. This leads to the selection of a cosine filter as shown in Eq. 1.

$$h(n) = \cos\left(n \cdot \frac{f_c}{f_s} \cdot 2\pi\right) + 1 \quad (1)$$

The filter  $h$  is a function of the number of filter steps  $n$ , which is an integer value, building a symmetric window around zero. The range of  $n$  depends on the chosen filter length.

The following factors are the cut-off frequency  $f_c$  and the sample frequency  $f_s$ .

For applying the filter some adjustments are needed. At first it will be normalised by using Eq. 2.

$$h(n) = \frac{h(n)}{\sum h(n)} \quad (2)$$

The function has to be cut at its first minimum to get a low-pass filter. Because of choosing a time discrete cosine function this cut off can be calculated by using Eq. 3 and Eq. 4.

$$T_c = \frac{f_s}{f_c} \quad (3)$$

$$-\frac{T_c}{2} \leq n \leq \frac{T_c}{2} \quad (4)$$

For every filter step  $n$  outside the defined window in Eq. 4 the filter is set to zero. The value  $T_c$  represents the period of the cosine.

The sample frequency  $f_s$  can be derived from the time difference between each bin of the histogram  $dt$ . For this analysis it is set to 10 seconds, but the number of bins can be varied leading to various time differences.

In Eq. 5 the relations are shown:

$$f_s = \frac{1}{dt} \quad (5)$$

The cut-off frequency has to be calculated for each specific re-entry analysis because it depends on the shape of the current satellite orbit and its remaining life time. For the calculation a Fast Fourier Transformation (FFT) is used. The result of applying the FFT on the Monte Carlo results will be called  $D(k)$ , with  $k$  as the frequency bin. Only the magnitude of  $D(k)$  has to be taken into account to determine the cut-off frequency. Furthermore the mean value is subtracted to remove the constant component of the signal.

The position of each maximum of  $|D(k)|$  can be used to calculate a cut-off frequency  $f_c$  by using Eq. 6 with the number of given bins  $N$ .

$$f_c = \frac{k_c \cdot f_s}{N} \quad (6)$$

Because the cut-off period ( $1/f_c$ ) is corresponding with the orbital period of the satellite it is used as a threshold for the smallest expected period as seen in Eq. 7. The aim is to find the frequency of the envelope and we suppose that it is not bigger than two times the orbit frequency of the satellite. The threshold was set to 0.475 of the satellite period to avoid the exclusion of cut-off frequencies which are slightly above 2.

$$T_c \geq 0.475 \cdot T_{\text{sat}} \quad (7)$$

An example for evaluating the cut-off frequency by using the FFT is shown in Fig. 4. The frequency bin  $k$  was plotted on the x-axis, the magnitude of  $D(k)$  on the y-axis.

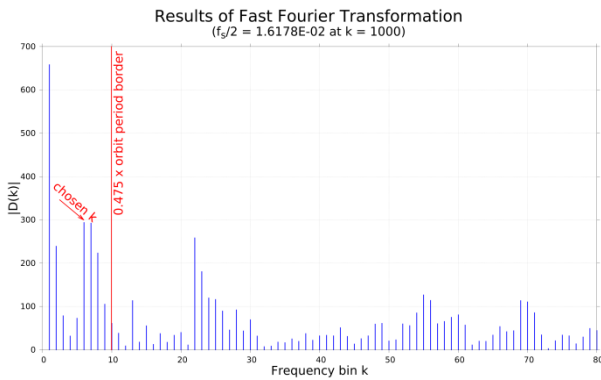


Figure 4. Magnitude of results of Fast Fourier Transformation used on Monte Carlo results

The chosen cut-off frequency derived by Eq. 6 will in the end be multiplied with a correction factor to improve the filtering results because the used cosine filter is not frequency-flat in the passband.

Applying the filter on the Monte Carlo results in the time regime  $d(n)$  is done by using Eq. 8 [2]. The result is the probability of re-entry  $p(n)$  in the time regime.

$$p(n) = \sum_{k=-\infty}^{\infty} h(k) \cdot d(n-k) \quad (8)$$

#### 1.4 Deriving the accumulated probability

After applying the filter on the Monte Carlo results as shown in Fig. 3 we get a smoothed curve of discrete probability of re-entry for a given time interval. The resolution of the probability is proportional to the bin size of the used histogram data, in this case 10 seconds.

This means we received a discrete function in the time domain (with a resolution of 10 seconds) for the probability of a re-entry, which will be called  $p(t)$ . In Fig. 5 the pure Monte Carlo results (green bars) and the smoothed probability curve (blue) are illustrated.

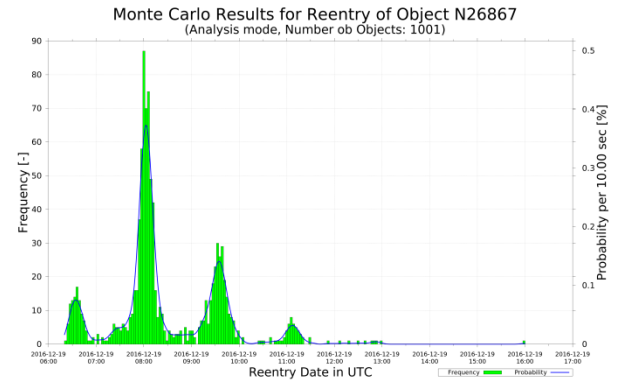


Figure 5. Pure Monte Carlo results of re-entry with smoothed probability curve

To calculate the re-entry probability for a defined time window the smoothed probability distribution has to be integrated to get the accumulated probability. Because we only have a discrete distribution and no function the bins are summed up in the interval of interest as shown in Eq. 9.

$$p_{\text{win}} = \sum_{t=t_{\text{start}}}^{t_{\text{end}}} p(t) \quad (9)$$

The value  $p_{\text{win}}$  is the probability for a given time window. To get the probability of re-entry for a certain area of interest the time window of the overflight has to be calculated. Analysing the data for this time window directly leads to the re-entry probability for a given area of interest

## 1.5 Utilisation of derived products

The derived probability density distribution can be used to reduce the probability of false alerts by setting a threshold for reporting a re-entry for an area of interest. Everything below a certain probability would be treated as not critical like it is done for collision avoidance.

In addition to this pure number further information on the re-entry probability along the remaining ground track can be provided to the operator. As supplement to the ground track shown in Fig. 1 a heat map based on the Monte Carlo results can be generated. Such a heat map shows the areas of higher re-entry probabilities directly to the operator. An example for such a graphic is shown in Fig. 6.

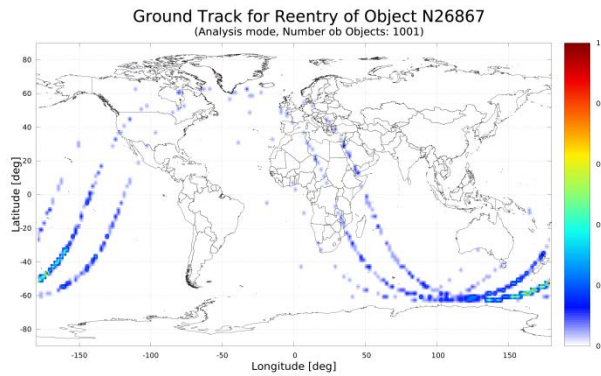


Figure 6. Heat map of re-entry Monte Carlo simulation

The colour code is normalised, thus the maximum is 1. This means for the dark red coloured areas (for this example with a resolution of  $2^\circ$  by  $2^\circ$ ) the most re-entries have been calculated. White colour means that no re-entry had been calculated for those areas.

This map can be directly used to show the operator that a re-entry over Europe is rather unlikely for this object.

## 2 RESULTS

The analysis mode was evaluated by applying the new re-entry propagator mode to several different re-entries. Different orbit types lead to characteristic probability distributions. For this paper an eccentric orbit was chosen to show the benefits of this method. The choice fell on MOLNIYA 3-51 (2001-030A), because it had some uncertainties in the TIP messages and illustrates well the benefits of the new analysis mode. Tab. 2 summarizes the orbital data for the satellite.

This is the basic information for the re-entry analysis mode. For this example one thousand additional Monte Carlo runs are executed. The state vector was varied in the position, building a cloud of vectors around the initial position.

Table 2. Satellite data for MOLNIYA 3-51

Name	Value
satellite name	MOLNIYA 3-51
International Designator	2001-030A
NORAD ID	26867
decay day	2016-12-19
decay time (TIP [3])	06:43:00
orbit data epoch	2016-12-18T23:45:22
Period	99.55 min
Inclination	$62.42^\circ$
Apogee	1400.09 km
Perigee	88.55 km
Eccentricity	0.09216

The used standard deviations are listed in Tab. 3. In the future it is planned to use covariance information from orbit determination and a relative variation of the ballistic coefficient to improve the results.

Table 3. List of used variations for re-entry analysis

Error	Value
Radial	1 km
Along-Track	4 km
Cross-Track	2 km

Fig. 1 shows that for this initial data there are two remaining overflights for the area of interest (EU). For calculating the re-entry probability we need the overflight times. With this data we can use the re-entry analysis mode and derive the probability for a re-entry over the given area of interest. The derived probability is referred to the duration of the overflight in seconds in order to get comparable results. This lead to the in Tab. 4 listed probabilities.

Table 4. Probability of re-entry for area of interest (EU)

#	Start	End	probability	rel. probability
1	07:24:21	07:32:55	0.0152	$2.96 \cdot 10^{-05}$ 1/s
2	09:04:01	09:05:36	0.0023	$2.42 \cdot 10^{-05}$ 1/s
$\Sigma$			0.0175	$2.87 \cdot 10^{-05}$ 1/s

We compared these values to a theoretical overflight during the maximum of the curve (see Fig. 5) at about 08:06:30 UTC to get a better feeling for the dimension of the values. The result is listed in Tab. 5.

Table 5. Probability of re-entry near maximum at 08:06:30 UTC

Start	End	probability	rel. probability
08:02:15	08:10:45	0.1259	$2.47 \cdot 10^{-04}$ 1/s

The derived probability is always corresponding with the remaining uncertainty. For this example a re-entry for the given area of interest is unlikely but still possible. A threshold for warnings has to be evaluated by analysing more re-entries to improve the forecasting concept. But already at this stage it is an improvement as additional information for the operator.

### 2.1 Improvement of predictions

In comparison to the currently used re-entry predictions during operations the new analysis mode provides more information to the operator. Besides the heat map and the re-entry probability for a given area of interest, which already provides more information than just using the ground track of a given uncertainty window, more information can be provided to the operator.

This additional information includes statistical values and the distribution of the Monte Carlo results in longitude and latitude. The statistical values are provided as numbers, the histogram data is provided as graphics.

Known uncertainties on the input parameters (e.g. covariance information from orbit determination) can be used to derive uncertainties for the re-entry besides using a window around the calculated COIW. Also the possible shift of the COIW between two revolutions is shown to the operator.

In Fig. 7 the Monte Carlo results for the last TLE are shown. The re-entry analysis predicts the re-entry one orbit revolution earlier at around 6:33 UTC (for comparison: last TIP predicts 6:43 UTC with a window of 31 minutes [3]).

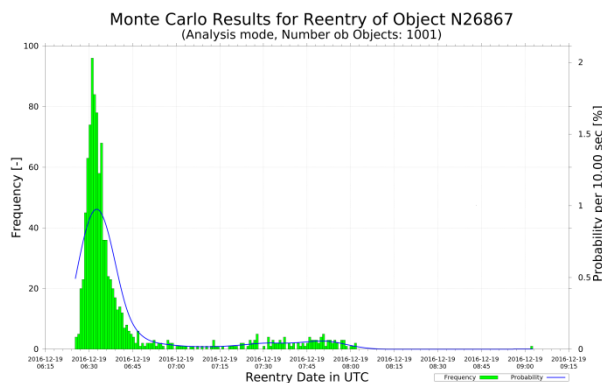


Figure 7. Monte Carlo results and probability distribution for last TLE

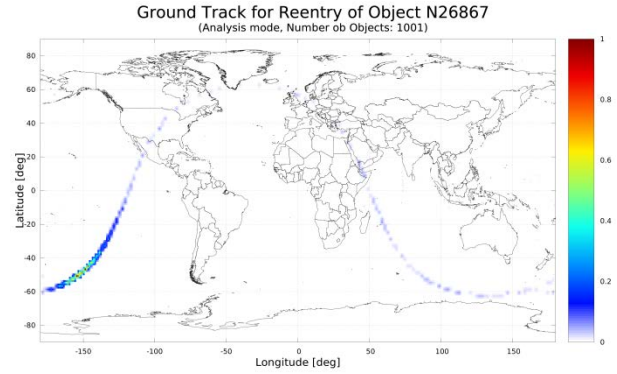


Figure 8. Heat map for last TLE

This COIW of re-entry can be seen in the earlier predictions, although it was not as likely as the prediction for one revolution later. The corresponding heat map is shown in Fig. 8. As already seen in in Fig. 2 there is no remaining risk of re-entry for the chosen area of interest.

### 3 CONCLUSION

Driven by the needs of operations for improving space situational awareness in the field of re-entry we built a new analysis mode for our re-entry propagator. This mode uses Monte Carlo simulations and filter techniques to calculate the probability of re-entry for a given area of interest.

Besides the probability the analysis of the Monte Carlo simulation also provides additional information to the operator, such as a heat map of the calculated re-entry points (in comparison to just using the ground track around the COIW with a given window of uncertainty) or statistical values.

The applied filter technique, a cosine filter with no negative samples, can be improved in the future to achieve a better fitting of the Monte Carlo results while still producing values above zero for the minima. But the used filter is an appropriate solution in the field of non-negative impulse response filter and leaned on the Hann function [4].

It is planned to change the fixed variations from the standard deviation to values derived from orbit determination and to use the variation of the ballistic coefficient in addition. The results of the current analysis show potential to improve the prediction and assessment of re-entries already and should be even more reliable with better input values.

In the future it will be possible to reduce the number of false alerts during operations by using the derived probability and setting a reliable threshold.

By automation of this process the operator will be provided with additional information to analyse the

situation. This process should start at around 1 day before the final re-entry to save computation time and still have enough time and data to react.

## REFERENCES

1. M. Eickmans (2015). Re-Entry Trajectory Analysis: Prediction of Uncontrolled Atmospheric Re-entry of Orbital Objects under Operational Aspects. In *Space Safety is No Accident*. Springer, Cham, Switzerland
2. U. Zölzer (2005). *Digitale Audiosignalverarbeitung (Informationstechnik)*. Vieweg + Teubner, Wiesbaden, Germany
3. <https://www.space-track.org> (as of 4 April 2017)
4. R. B. Blackman, J. W. Tukey (1959). Particular pairs of windows. In *The measurement of power spectra, from the point of view of communications engineering*. Dover, New York, USA, pp. 95–101